Solvation of the 2,5-Lutidyl Radical in Small van der Waals Clusters

J. A. Bray and E. R. Bernstein*

Department of Chemistry, Colorado State University, Fort Collins, Colorado 80523-1872

Received: August 24, 1998; In Final Form: October 14, 1998

The one-to-one clusters of the 2,5-lutidyl radical [2-CH_3,5-($\dot{C}H_2$)C_5H_3N] with Ar, N_2, CH_4, CF_4, C_2H_6, C_3H_8, C_4H_{10}, and C_2H_4 are studied by fluorescence excitation spectroscopy, mass resolved excitation spectroscopy, and ab initio and semiempirical calculational techniques. Cluster binding energies for the ground (D_0) and excited (D_1) states, cluster spectroscopic shifts, and van der Waals cluster vibrational modes are reported for these systems. The agreement between the observed and calculated cluster properties is quite good. Unlike the benzyl radical, the 2,5-lutidyl radical does not react with ethylene in its D_1 excited electronic state.

Introduction

Intermolecular interactions in the condensed phase can have controlling influences on the properties and chemistry of stable molecules and reactive intermediates. Geometries, dynamics, transition states, reaction paths, and even mechanisms can be affected by the presence of a solvation shell surrounding a particular dilute species. Radicals can be especially susceptible to such solvation perturbations, and their properties and behavior can be greatly influenced by their surroundings. Studies of these intermolecular interactions for both the ground and excited states of radicals range from direct investigations of solution radical properties and behavior to model studies of supersonic jet expansion cooled van der Waals clusters containing a radical solvated by from one to may ($1 \leq n \leq 100$) solvent species (i.e., R·(Solv)$_n$). A great deal of effort has been expended over the past 20 years in the study of stable molecules solvated in van der Waals clusters:[1−20] cluster structure, bonding energies, spectroscopic shifts, dynamics, and chemical reactions (electron and proton transfer) have been explored for these closed-shell molecular systems.

Solvation properties, dynamics, and chemistry are even more important for reactive intermediates as they can often be quite difficult to study in the condensed phase. Cluster studies of open-shell systems thus become more central to the elucidation of the behavior radicals and other reactive intermediates. In the past few years, cluster studies on a number of radical species have appeared: benzyl ($C_6H_5CH_2$),[21,22] methoxy (CH_3O),[23−25] cyanate (NCO),[25,26] cyclopentadienyls (C_6H_4X = Xcpd, X = H, CH_3, F, CN).[25,27−30] In pursuing these radical solvation studies further, we have generated the 3-picolyl [from 3-methylpyridine, 3-($\dot{C}H_2$)C_5H_4N] and 2,5-lutidyl [from 2,5-dimethylpyridine, 2-(CH_3),5-($\dot{C}H_2$)C_5H_3N] radicals that are analogues of benzyl and xylyl radicals,[31] respectively. The dynamics of the excited D_1 state 3-picolyl radical are such that cluster spectra could not be observed in our experiments by either mass or fluorescence detection for this radical. The 2,5-lutidyl radical is generated by photolysis of 2,5-dimethylpyridine, lutidine, which removes a hydrogen from the 5-methyl group. This study demonstrates that the various substitutions on the benzyl radical moiety (a nitrogen atom for a carbon atom in the ring and an additional methyl group at the 2 position) significantly affect the electronic structure, dynamics, and photochemistry of these radicals. The clusters reported in this work are one-to-one clusters of the 2,5-lutidyl radical with Ar, N_2, CF_4, CH_4, C_2H_6, C_3H_8, C_4H_{10}, and C_2H_4. Experimental results include cluster spectroscopic shifts and general limits on or ranges for the cluster binding energies of these clusters. From these data, we conclude that the D_1 electronic excited state of this radical is not close to the excited D_2 state as found for the benzyl radical ($E(D_2) - E(D_1) \sim 500$ cm^{-1}).[32−34] Atom−atom potential energy calculations yield ground- and excited-state binding energies for these clusters, the cluster structure, and spectroscopic shifts. Based on a harmonic force field derived from these potential energy surfaces, the ground- and excited-state van der Waals (vdW) modes are calculated and the low-energy bending modes are found to be in good agreement with vdW mode features in the spectra of these clusters.

Procedures

Experiment. The 2,5-lutidyl radical is generated photolytically. Our experimental technique for detection and generation of supersonically cooled radicals and their clusters has been described previously.[21,27] The expansion pressure used in these studies is ca. 80 psi. The clustering species or solvent (Ar, CH_4, CH_4, ...) is added to the He expansion gas at ∼10% to reach this backing pressure.

Mass-resolved excitation spectra of these clusters are obtained by placing a 97% pure sample of 2,5-dimethylpyridine (2,5-lutidine, Aldrich) in the sample chamber of an R. M. Jordan pulse valve operating at 10 Hz. The sample is heated slightly to increase the concentration of the precursor in the expansion gas. Two SRS DG535 digital delay generators are used to control the precise timing of the three lasers: an ArF excimer laser for photolysis and two Nd:YAG pumped dye lasers for excitation and ionization of the radical clusters. These delay generators also control the timing of the pulsed nozzle. The dye for $D_1 \leftarrow D_0$ excitation of the radical is courmarin 460 (Exciton), and for the $I \leftarrow D_1$ transition of the radical, the dye employed is LDS 698 (doubled and mixed with the Nd:YAG fundamental) to produce photons at 39 682 cm^{-1}. Independent timing control of the nozzle and all lasers in the experiment allows one to optimize each part of the experimental process independently. Temporal separation of the two spectroscopic lasers is ca. 40 ns, which is well within the 250-ns lifetime of the 2,5-lutidyl D_1 state.

The signal intensity of the 2,5-lutidyl radical clusters is somewhat weak due in part to the low intensity of the ionization

10.1021/jp983458k CCC: $18.00
Published on Web 01/15/1999

laser. The average power of the ionization laser is ~800 μJ/pulse compared to the excitation laser whose power is ~ mJ/pulse. To enhance the signal, the ~1-cm-diameter ionization beam is gently focused to a spot size of ~2−3 mm in the ionization region. The combination of low power and small spot size produces small signals: maximum signal intensity for the 2,5-lutidyl radical clusters is ~5 mV. Compare these values to the 30−400-mV signals detected for the benzyl radical clustered with nonpolar solvents.[21]

Two of the solvent clusters, Ar and CF_4, are not detected by mass-resolved excitation spectroscopy but are detected instead using fluorescence excitation spectroscopy. This latter experimental configuration is similar to that used to detect mass spectra, but the ionization laser is not employed. Other differences in the experimental configuration include the photolysis alignment and the placement of the excitation laser relative to the nozzle. Photolysis for the fluorescence excitation (FE) experiment is performed with the ArF laser beam collinear to the molecular beam, while it makes an angle of ~30° relative to the beam axis for the mass detection experiment. The excitation laser intersects the molecular beam ~1.5 cm from the nozzle in the FE experiment, while it intersects the molecular beam ~15 cm from the nozzle in the mass detection experiment. The relatively weak signals generated in both the mass-resolved and fluorescence excitation experiments prevent us from performing assignment diagnostic experiments such as hole burning. The fluorescence intensity observed for the 2,5-lutidyl radical and clusters is about 10 times weaker than the comparable benzyl radical signal intensities, probably due to enhanced radiationless decay channels for the pyridine-based systems.

Theoretical Section. Calculations involving both ab initio quantum chemistry and empirical atom−atom potentials are used in order to interpret and understand the experimental spectra obtained for each of the clusters. To interpret the spectra of the 2,5-lutidyl radical clusters, three specific pieces of information are important: cluster structure, cluster ground- and excited-state binding energies, and the van der Waals vibrational mode energies in the cluster excited state. This information can be obtained from the empirical atom−atom potential energy functions for the ground and excited electronic states of the cluster. The approach taken to these calculations and the use of potential energy functions to calculate the experimental observables has been recently discussed in detail.[7,27−29] In order to determine these potential functions, partial atomic charges, polarizabilities, and van der Waals radii for the atoms of the cluster in both electronic states of the radical are required. To obtain atomic charges and the radical structure, ab initio calculations are performed on an IBM RISC/6000 computer running the GAUSSIAN 94 molecular orbital package.[35] The partial charges and the structure of the 2,5-lutidyl radical presented in this section are the result of a (7 × 7) complete active space self-consistent-field (CASSCF) calculation using the d95** basis set. The six π orbitals of the pyridine ring and the p orbital of the radical carbon are selected as the active space. Because the first excited electronic state is generated by a $\pi^* \leftarrow$ n transition, the methyl rotor is not included in the CAS space energy minimization and is allowed to roatate freely. No geometry constraints are placed on the 2,5-lutidyl radical for the calculations.

The resultant geometry for the 2,5-lutidyl radical is planar with the exception of the two hydrogen atoms on the methyl group which lie above and below the plane of the radical. Calculations confirm that this radical has C_s symmetry. The optimized geometry and the coordinate axis for the 2,5-lutidyl radical are shown in Table 1.

TABLE 1: 2,5-Lutidyl Radical Charges and Parameters for Atom−Atom Potentials[a]

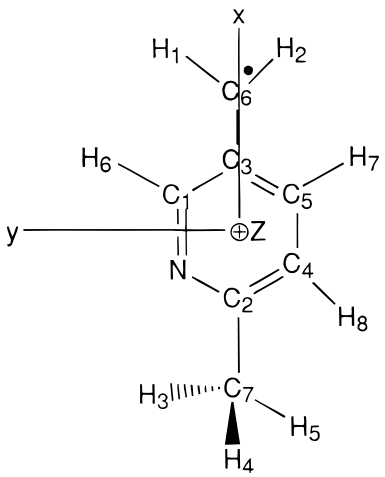

	atomic charges		D_0		D_1	
atom	D_0	D_1	α_i	$2r_i$	α_i	$2r_i$
N	−0.642 792	−0.668 979	0.930	2.92	1.005	3.685
C_1	0.221 432	0.241 011	1.150	3.70	1.130	3.550
C_2	0.726 307	0.645 999	1.150	3.70	1.130	3.550
C_3	0.111 627	0.244 136	1.150	3.70	1.142	3.600
C_4	−0.476 785	−0.356 249	1.150	3.70	1.142	3.600
C_5	−0.040 379	−0.156 846	1.150	3.70	1.142	3.600
C_6	−0.446 120	−0.483 863	1.150	3.70	1.165	3.755
C_7	−0.549 428	−0.521 512	0.930	4.120	0.930	4.120
H_1	0.155 925	0.162 630	0.420	2.930	0.420	2.930
H_2	0.170 656	0.172 167	0.420	2.930	0.420	2.930
H_3	0.128 730	0.113 114	0.420	2.920	0.420	2.920
H_4	0.139 087	0.133 038	0.420	2.920	0.420	2.920
H_5	0.139 239	0.133 044	0.420	2.920	0.420	2.920
H_6	0.065 578	0.063 478	0.420	2.930	0.420	2.930
H_7	0.122 697	0.130 372	0.420	2.930	0.420	2.930
H_8	0.174 045	0.148 459	0.420	2.930	0.420	2.930

[a] All H atoms are calculated with a polarizability, α_i = .420 Å^3. Twice the van der Waals radii, $2r_i$ = 2.920 Å or $2r_i$ = 2.930 Å depending upon its connection to an sp^3 or sp^2 carbon, respectively. Hydrogen atom parameters are assumed not to change from D_0 to D_1. The electrostatic potential grid method is used to calculate the charges as discussed in ref 36. Atom numbering is displayed for ab initio calculational purposes only.

Partial charges for each of the atoms are obtained using the same level of theory as stated above and a C_s symmetry-optimized geometry. An electrostatic potential grid technique is used to determine the partial charges for each of the atoms.[36] Table 1 shows the 2,5-lutidyl radical atoms with the calculated charges for both the ground and excited states. The nitrogen and carbon atoms nearest the radical carbon increase their charges upon excitation, whereas the carbon atoms on the opposite wide of the ring tend to lose electron density.

Cluster structures and binding energies are calculated using an atom−atom Lennard-Jones−Coulomb potential energy function

$$E = \sum_{i=1}^{n}\sum_{i=1}^{m}\left\{\left(\frac{A_{ij}}{r_{ij}^{12}} - \frac{C_{ij}}{r_{ij}^{6}}\right) + \frac{q_i q_j}{D r_{ij}}\right\} \qquad (1)$$

in which

$$A_{ij} = C_{ij} r_{\min}{}^6/2 \qquad C_{ij} = \frac{{}^3/_2 e(\hbar/m^{1/2})\alpha_i\alpha_j}{(\alpha_i/N_i)^{1/2} + (\alpha_j/N_j)^{1/2}} \qquad (2)$$

The symbols in these equations are defined as follows: m, the electronic mass; q_i and q_j, the atomic partial charges; D, the dielectric constant which is equal to one in a vacuum (however the potential parameters are derived from condensed phase data; hence, $D = 2$ is often used); $r_{\min}$, the sum of van der Waals radii for atoms i and j, $r_{\min} = r_i + r_j$; α_i, the polarizability for that atom; N_i, the effective number of electrons; and r_{ij}, the distance between atom i and atom j of different molecules.[37−40] Hydrogen bonding is not considered in the potential specified above but can easily be included if the systems studied have a hydrogen bonding interaction.

The potential energy function in eq 1 is used to determine both cluster binding energy and cluster structure. The cluster structure is optimized by minimizing the calculated binding energy. For these calculations to be meaningful, good parameters ($r_{\min}$, q_i, and α_i) are essential. Ground-electronic-state van der Waals parameters (α_i and r_i) are obtained for the C, N, and H atoms of the cluster as given in the literature.[37−40] Charges for both the ground- and excited-state radicals are taken from ab initio calculations. Excited state atomic polarizabilities and vdW radii are fit to reproduce the cluster spectroscopic shift of the 2,5-lutidyl radical−$(Ar)_1$ cluster.[21,27−29] Due to the low symmetry of the radical chromophore and the large variation of its partial atomic charges with the electronic state of the radical (see Table 1), α_i and r_i are obtained for all heavy atoms of the excited-state radical. Although we allow for large flexibility in the adjustment of excited-state atomic polarizabilities and vdW radii, the parameters for most carbons are unchanged from those employed in the benzyl radical calculations.[21] The majority of the fitting changes are for the two carbons directly connected to the ring nitrogen atom. These binding energies are electronic in nature and do not account for vibrational zero-point motion in the potential wells. On the basis of experience with both stable molecules and radicals, one can expect such calculated binding energies to be accurate to ca. 10−15%.[1,2,6,21,22,24,26,30]

The vdW modes are determined from the calculated cluster potential energy surfaces employing a normal-mode analysis and a harmonic oscillator potential approximation for both the ground and excited states.[41,42]

Results

The mass-resolved excitation spectrum for the 2,5-lutidyl radical is shown in Figure 1 so that it may be used as a reference for the clusters discussed. The important features to note are the four intense ones given as 21 395 (0_0^0), 21 801 ($6a_0^1$), 21 938 ($6b_0^1$), and 22 215 cm^{-1} (1_0^1). These intense features will be used to estimate an upper bound on the cluster binding energies; their assignments are discussed in the first paper of this series.[43] As mentioned previously, the cluster signal intensity is very low, so only cluster features associated with the most intense chromophore transitions can be observed. Calculations for this molecule indicate that only one excited electronic state (D_1) exists at ∼22 000 cm^{-1}.

The cluster spectroscopic shifts, $E_{\text{cluster}}(0_0^0) - E_{\text{radical}}(0_0^0) \equiv \Delta E$, are negative for all clusters. These values are summarized in the right-hand column of Table 2. The red shifts are somewhat larger than the corresponding red shifts observed for benzyl radical nonpolar solvent molecule clusters,[21] but are significantly less than the shifts reported for substituted cyclopentadienyl radical nonpolar solvent clusters.[27]

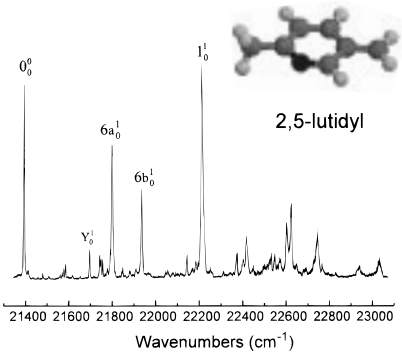

Figure 1. Mass-resolved excitation spectrum of the 2,5-lutidyl radical and the calculation radical geometry. Vibronic assignments are given as presented in the text and the preceding paper in this issue.[43]

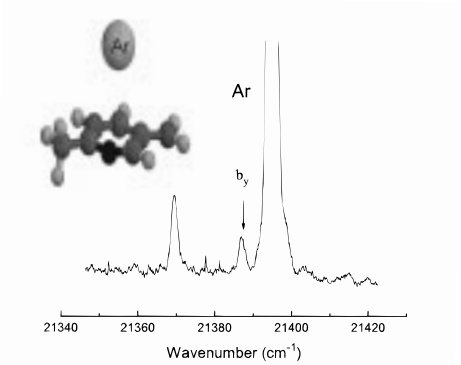

Figure 2. Fluorescence excitation spectra of the 2,5-lutidyl radical−$(Ar)_1$ cluster. The calculated cluster geometry is also pictured.

TABLE 2: Binding Energies and Spectroscopic Shifts (ΔE) for the 2,5-Lutidyl Radical Clustered with Various Nonpolar Solvents (in cm^{-1})

	binding energy		ΔE	
solvent	ground state	excited state	calcd	obsd
Ar	483.2	509.03		−26
N_2	606.1	644.3	−38.2	−40
CF_4	998.7	1045.0	−46.3	−34
CH_4	616.2	644.3	−28.2	−57
C_2H_6 (1)	835.9	868.1	−32.3	−93
C_2H_6 (2)	706.3	734.9	−28.6	−61
C_3H_8	1085.7	1152.5	−66.8	−105
C_4H_{10}	1297.5	1352.1	−54.6	−117
C_2H_4	953.2	1005.9	−52.7	−78

2,5-Lutidyl−$(Ar)_1$. Figure 2 shows the vibronic spectrum of the 2,5-lutidyl radical−$(Ar)_1$, $LR(Ar)_1$, cluster origin as detected using fluorescence excitation spectroscopy. Also shown in Figure 2 is the calculated geometry for this cluster. The bare radical origin is amplified to show the two cluster features. No other features are observed to be built on any of the other 2,5-lutidyl radical features. The absence of higher energy cluster vibronic transitions supports the calculational result that only one electronic state for the 2,5-lutidyl radical lies in the neighborhood of 22 000 cm^{-1}. This observation additionally supports the assignment of the peak at 22 215 cm^{-1} as 1_0^1 D1 ← D_0. The $LR(Ar)_1$ cluster has its $D_1 \leftarrow D_0$ electronic transition origin at 21 369 cm^{-1}, which is 26 cm^{-1} red-shifted from the bare radical 0_0^0.

Similar to other conjugated π systems, the calculated cluster structure places the Ar atom directly above the ring and slightly shifted toward the nitrogen atom. One other cluster geometry with the Ar facing the methyl rotor is calculated to be a minimum; however, this configuration for the Ar cluster has a much lower binding energy (∼200 cm^{-1}) and has a very narrow

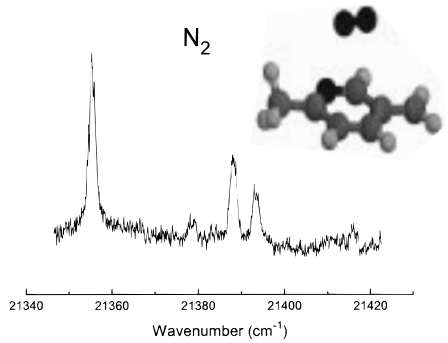

Figure 3. Mass-resolved excitation spectrum of the 2,5-lutidyl radical−$(N_2)_1$ cluster at the cluster 0_0^0 transition. The calculated cluster geometry is also pictured.

range of entrance channels, only forming in about 10% of the random starting geometries chosen by the calculational algorithm. Using the most probable structure, the excited-state parameters for the chromophore are adjusted so that the experimental and calculated shifts are identical. The approach taken to this fitting is elaborated in refs 21 and 27.

Cluster vibrations can be assigned based on calculations involving the Lennard-Jones−Coulomb potential outlined in eqs 1 and 2 and Table 2.[42] For the present clusters, the vibrations are ordered as $E(b_y) < E(b_x) < E(\sigma)$ (see Table 1 for axes). We thus assign the second cluster feature at $0_0^0 + 15.7$ cm^{-1} in Figure 2 to be the b_{y0}^1 transition of the LR(Ar)$_1$ cluster. The calculated value of this mode is 17.4 cm^{-1}. The σ^1 and b_x^1 modes are calculated to have an energy of 50.7 and 31.3 cm^{-1}, respectively.

2,5-Lutidyl−$(N_2)_1$. The mass-resolved excitation spectrum of the LR$(N_2)_1$ cluster is presented in Figure 3. The cluster origin lies at 21 355 cm^{-1}, and its associated vdW mode transitions are observed at $0_0^0 + 24$ cm^{-1}, $0_0^0 + 34$ cm^{-1}, and $0_0^0 + 37$ cm^{-1}. The calculated structure for this cluster is presented in the figure. In this geometry, the N_2 molecule lies above the ring and is roughly centered at a distance of ∼3.1 Å from the ring plane. The calculated cluster binding energy and shift are given in Table 2. The calculated and observed shifts are nearly identical.

The calculated vdW vibrational modes for this clusters are 24.0, 32.8, and 67.9 cm^{-1} corresponding to b_y, b_x, and σ. The vdW vibrational modes can be tentatively assigned as b_y and b_x for the observed modes at 24 and 34 cm^{-1}, respectively. The observed mode at ∼37 cm^{-1} cannot be assigned directly to a pure bending mode. A low-energy rotational motion about the cluster z axis can be expected for the N_2 molecule.[6,13,44]

2,5-Lutidyl−$(CF_4)_1$. The fluorescence excitation spectrum of the LR$(CF_4)_1$ cluster is displayed in Figure 4. Two cluster features are observed: one at 21 361 cm^{-1} (0_0^0) and one at 21 377 cm^{-1} (b_{y0}^1). The cluster spectroscopic shift is −34 cm^{-1} (see Table 2) and the vibrational energy of b_y^1 is 18 cm^{-1}. The calculated shift value is −46 cm^{-1}, and the vibrational mode b_y^1 is calculated to be ∼22 cm^{-1}.

Because of the large electron density and partial charges on the fluorine atoms of CF_4, one would expect that the LR$(CF_4)_1$ cluster would have large binding energies in the D_0 and D_1 electronic states. These binding energies are ∼1000 and ∼1045 cm^{-1}, respectively, and they strongly reflect the interaction between the fluorine atoms and the pyridine ring π-electron system. The CF_4 molecule lies above the aromatic plane with three fluorine atoms closest to the ring. The CF_4 molecule has a low barrier to rotation about the cluster z axis that lies along the C−F bond that points away from the ring.

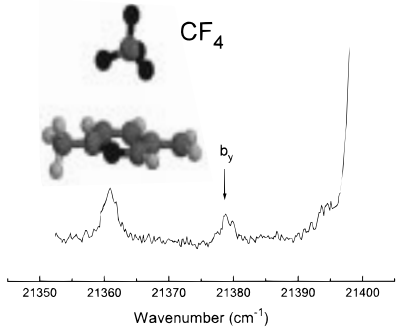

Figure 4. Fluorescence excitation spectrum of the 2,5-lutidyl radical−$(CF_4)_1$ cluster. The calculated cluster geometry is also pictured.

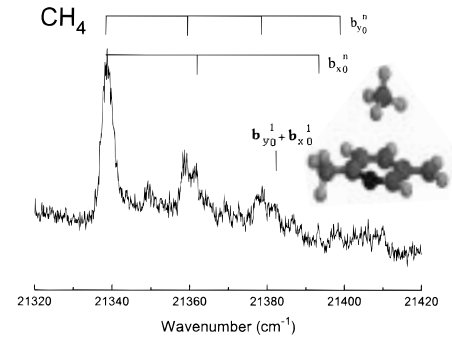

Figure 5. Mass-resolved excitation spectrum of the 2,5-lutidyl radical−$(CH_4)_1$ cluster. The calculated cluster geometry is also pictured.

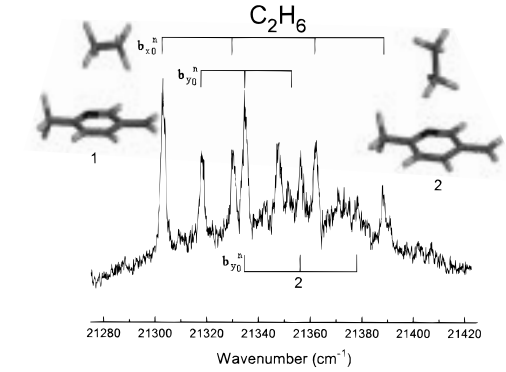

Figure 6. Mass-resolved excitation spectrum of the 2,5-lutidyl radical−$(C_2H_6)_1$ cluster. The calculated cluster geometry is also pictured.

2,5-Lutidyl−$(CH_4)_1$. The mass-resolved excitation spectrum of the LR$(CH_4)_1$ is displayed in Figure 5 along with the calculated cluster structure. The spectroscopic shift for the cluster is −57 cm^{-1} (0_0^0 transition at 21 338 cm^{-1}) and two vibrational modes, b_x^1 and b_y^1, along with their progressions and a combination band are identified: $b_y^1 = 19$ cm^{-1} and $b_x^1 = 22$ cm^{-1}.

The cluster structure is the standard one described for the LR$(CF_4)_1$ cluster. The methane molecule can undergo nearly free rotation above the aromatic ring plane and can translate parallel to the plane (b_x and b_y) with large amplitude displacements.

The cluster binding energies for the D_0 and D_1 electronic states of the radical are calculated to be 616 and 644 cm^{-1}, giving a calculated cluster spectroscopic shift of −28 cm^{-1}. This value is about one-half the observed one. The calculated b_x^1 and b_y^1 vdW modes are 29.3 and 19.2 cm^{-1}, respectively.

2,5-Lutidyl−$(C_2H_6)_1$. The LR$(C_2H_6)_1$ cluster spectrum is displayed in Figure 6 along with the two calculated cluster geometries. The spectrum obtained is assigned to two clusters

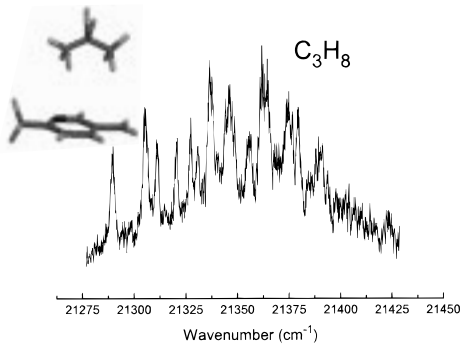

Figure 7. Mass-resolved excitation spectrum of the 2,5-lutidyl radical−$(C_3H_8)_1$ cluster. The calculated cluster geometry is also pictured.

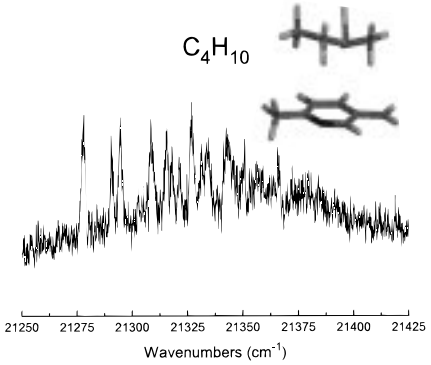

Figure 8. Mass-resolved excitation spectrum of the 2,5-lutidyl radical−$(C_4H_{10})_1$ cluster. The calculated cluster geometry is also pictured.

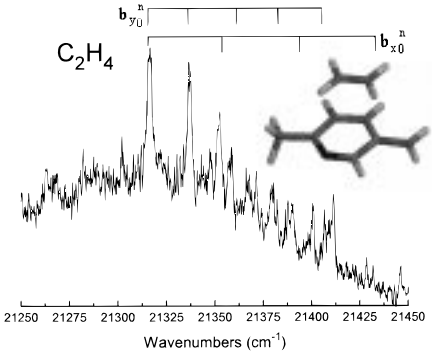

Figure 9. Mass-resolved excitation spectrum of the 2,5-lutidyl radical−$(C_2H_4)_1$ cluster. The calculated cluster geometry is also pictured.

based on these calculations and the fact that benzene, toluene, and benzyl radical/ethane clusters also display two structures.[21,45,46] The lower energy cluster origin is at 21 302 cm^{-1}, red-shifted 93 cm^{-1} from the parent radical origin at 21 395 cm^{-1}. The second cluster structure is suggested to have its origin transition at 21 334 cm^{-1}. The calculated cluster structure 1 is assigned to the lower energy origin, and the calculated cluster structure 2 is assigned to the higher energy origin. The assignments are based simply on the cluster binding energies: the larger binding energy should have the larger shift. The calculated shifts for these clusters are similar and quite small compared to those observed. They are given in Table 2. The parallel (1) and perpendicular (2) calculated cluster structures are similar to those found for the benzene and toluene $(C_2H_6)_1$ clusters.

Vibrational mode calculations for the two cluster structures yield (1) $b_x^1 = 26.7$ cm^{-1} and $b_y^1 = 18.6$ cm^{-1} with those observed at 29 and 16 cm^{-1}, respectively, and (2) $b_y^1 = 20.4$ cm^{-1} calculated and 22 cm^{-1} observed. Agreement between the calculated and observed vdW bending modes is quite good.

2,5-Lutidyl−$(C_3H_8)_1$. The LR$(C_3H_8)_1$ cluster mass-resolved excitation spectrum is quite complex as displayed in Figure 7 for the origin transition. Aside from the system origin transition at 21,290 cm^{-1} the other features are difficult to assign in this spectrum because many cluster conformations are anticipated. As pointed out above, the spectra of these clusters are too weak (ca. 5 mV) to allow definitive hole-burning studies, which could identify cluster isomers, to be done.[47] The D_0 and D_1 binding energies for the most stable LR$(C_3H_8)_1$ cluster conformation are 1085.7 and 1152.5 cm^{-1}, respectively. This structure is presented in Figure 7, and it is typical for planar aromatic systems.[6] The three carbon atoms of propane lie in a plane perpendicular to the plane of the radical aromatic ring, with the central propane carbon atom shifted toward the radical moiety.

The spectroscopic shift for this cluster is −105 cm^{-1}, and the calculated value is −66.8 cm^{-1}. The excited-state cluster binding energy seems to be underestimated by our present series of approximations for the potential energy function as the solvent molecule increases in size and becomes more polarizable.

2,5-Lutidyl−$(C_4H_{10})_1$. The spectrum and structure calculated for the butane cluster is quite similar to that found for the propane (Figure 8). The spectrum origin lies at 21 278 cm^{-1}, and the observed cluster spectroscopic shift is −117 cm^{-1}. The largest cluster binding energies for the D_0 and D_1 states are 1297.5 and 1352.1 cm^{-1}, respectively. The calculated cluster shift is again small, −54.6 cm^{-1}, presumably due to an underestimation of the D_1 binding energy. Table 2 summarizes all these results. Many other isomers of this cluster can be calculated; most have the butane molecule in a different orientation with respect to the in-plane axes of the lutidyl radical.

2,5-Lutidyl−$(C_2H_4)_1$. Benzyl radical $(C_2H_4)_{1,2}$ clusters have been shown to undergo a reaction in the D_1 excited state of the radical based on both experimental observation and ab initio calculations.[22] One might anticipate that such addition chemistry would also take place for the substituted benzyl radical analogue 2,5-lutidyl clustered with ethylene. The experimental signatures for this reaction for the benzyl−$(C_2H_4)_1$ cluster are very broad spectra that continue for more than 15 000 cm^{-1}, a red shift in the onset of this spectrum, and a lowered ionization energy.[21,22] As can be seen in Figure 9, the spectrum of the lutidyl−$(C_2H_4)_1$ cluster is sharp, extends for only about 100 cm^{-1}, and can be assigned as due to two short progressions (b^n_{y0} and b^n_{x0} with $b_y^1 = 21$ cm^{-1} and $b_x^1 = 38$ cm^{-1}). These modes are calculated to lie at $b_y = 21$ cm^{-1} and $b_x = 39$ cm^{-1}. The cluster shift is observed as −78 cm^{-1} and calculated from the binding energies to be −52.7 cm^{-1}. The D_0 and D_1 binding energies are 953.2 and 1005.9 cm^{-1}, respectively.

The broad weak background for this spectrum is only 2-4 mV and probably arises from fragmentation of larger clusters.

Discussion

The spectral shifts for solvents referred to herein are larger than the trends presented for the benzyl radical but smaller than those of the Xcpd radicals (X = CH_3, CN, F). The calculated spectral shifts are qualitatively correct for all clusters. The parameters for the excited-state atoms are not known from other data sets, and hence, adjusting excited-state parameters to match the spectral shift of the argon cluster limits the accuracy of these calculations. Nonetheless, the excited-state bending modes are generally well represented by a harmonic projection of the excited-state potential energy surface.

Small changes in the polarizability and vdW radii do not have a significant effect on the overall minimum geometry, and the calculated cluster structures appear to be quite reasonable. These structures in turn provide the vdW frequencies used to assign the spectra.

Conclusion

In this work, we have shown that the 2,5-lutidyl radical solvation by nonpolar molecules can be relatively well modeled by Lennard-Jones−Coulomb potential energy surfaces for both the ground and excited electronic states of the radical with regard to cluster structure, binding energies, spectroscopic shifts, and van der Waals vibrational modes. While the 2,5-lutidyl radical is similar to the benzyl radical in these properties, it does not obviously display the D_1 addition chemistry found for the benzyl radical $(C_2H_4)_1$ cluster reported earlier.[22] A barrier must exist for this reaction for the lutidyl radical in both the ground and excited electronic states.

Acknowledgment. This work was supported in part by the USNSF and USARO.

References and Notes

(1) (a) *Chemical Reactions in Clusters*; Bernstein, E. R., Ed.; Oxford: New York, 1996. (b) *Atomic and Molecular Clusters*; Bernstein, E. R., Ed.; Elsevier: New York, 1990. (c) *Chem. Rev.* **1994**, *94* (7). (d) *J. Chim. Phys.* **1995**, *92* (2). (e) *Chem. Rev.* **1986**, *86* (3). (f) Foster, S. C.; Miller, T. A. *J. Phys. Chem.* **1989**, *93*, 5986.

(2) (a) Kim, S. K.; Bernstein, E. R. *J. Phys. Chem.* **1990**, *84*, 3531. (b) Kim, S. K.; Li, S.; Bernstein, E. R. *J. Chem. Phys.* **1991**, *95*, 3119.

(3) Li, S.; Bernstein, E. R. *J. Chem. Phys.* **1992**, *97*, 104.

(4) Li, S.; Bernstein, E. R. *J. Chem. Phys.* **1992**, *97*, 7383.

(5) Hineman, M. F.; Bernstein, E. R.; Kelley, D. F. *J. Chem. Phys.* **1993**, *98*, 2516.

(6) Sun, S.; Bernstein, E. R. *J. Chem. Phys.* **1996**, *100*, 13348.

(7) Dion, C. F.; Bernstein, E. R. *J. Chem. Phys.* **1996**, *104*, 2891.

(8) Fernandez, J. A.; Bernstein, E. R. *J. Chem. Phys.* **1997**, *106*, 3029.

(9) Wanna, J.; Bernstein, E. R. *J. Chem. Phys.* **1987**, *86*, 6707.

(10) Wanna, J.; Menapace, J. A.; Bernstein, E. R. *J. Chem. Phys.* **1986**, *85*, 1795.

(11) Wanna, J.; Bernstein, E. R. *J. Chem. Phys.* **1986**, *84*, 927.

(12) Breen, P. J.; Bernstein, E. R.; Seeman, J. I.; Secor, H. V. *J. Phys. Chem.* **1989**, *93*, 6731.

(13) Nowak, R.; Menapace, J. A.; Bernstein, E. R. *J. Chem. Phys.* **1988**, *89*, 1309.

(14) Webber, T.; Smith, A. M.; Riedle, E.; Neusser, H. J.; Schlag, E. W. *Chem. Phys. Lett.* **1988**, *175*, 79.

(15) Ohshima, Y.; Kohguchi, H.; Endo, Y. *Chem. Phys. Lett.* **1991**, *184*, 21.

(16) Felker, P. M.; Maxton, P. M.; Schaeffer, M. W. *Chem. Rev.* **1994**, *94*, 1787.

(17) Venturo, V. A.; Felker, P. M. *J. Chem. Phys.* **1993**, *99*, 748.

(18) Ebata, T.; Hamakado, M.; Moriyama, S.; Morioka, Y.; Ito, M. *Chem. Phys. Lett.* **1992**, *199*, 33.

(19) Saigusa, H.; Sun, S.; Lim, E. C. *J. Chem. Phys.* **1992**, *97*, 9072.

(20) Wittmeyer, S. A.; Topp, M. R. *Chem. Phys. Lett.* **1989**, *163*, 261.

(21) Disselkamp, R.; Bernstein, E. R. *J. Chem. Phys.* **1993**, *98*, 4339.

(22) Disselkamp, R.; Bernstein, *J. Phys. Chem.* **1994**, *98*, 7260.

(23) Powers, D. E.; Hopkins, J. B.; Smalley, R. E. *J. Phys. Chem.* **1981**, *85*, 2711.

(24) Fernandez, J. A.; Yao, J.; Bernstein, E. R. *J. Chem. Phys.* **1997**, *107*, 3363.

(25) Fernandez, J. A.; Yao, J.; Bray, J. A.; Bernstein, E. R. In *Structure and Dynamics of Excited States*; Laane, J., Ed.; Springer Verlag: Amsterdam, in press.

(26) Yao, J.; Fernandez, J. A.; Bernstein, E. R. *J. Chem. Phys.* **1997**, *107*, 8813.

(27) Fernandez, J. A.; Yao, J. Bernstein, E. R. *J. Chem. Phys.*, in press.

(28) Fernandez, J. A.; Yao, J. Bernstein, E. R. *J. Chem. Phys.*, in press.

(29) Fernandez, J. A.; Yao, J.; Bernstein, E. R. *J. Chem. Phys.*, in press.

(30) (a) Sun, S.; Bernstein, E. R. *J. Chem. Phys.* **1995**, *103*, 4447. (b) Yu, L.; Williamson, J.; Foster, S. C.; Miller, T. A. *J. Chem. Phys.* **1992**, *97*, 5273.

(31) Lin, T. Y. D.; Miller, T. A. *J. Phys. Chem.* **1990**, *94*, 3554.

(32) Fukushima, M.; Obi, K. *J. Chem. Phys.* **1990**, *93*, 8488.

(33) Eiden, G. C.; Weisshaar, J. C. *J. Chem. Phys.* **1996**, *104*, 8896.

(34) Cosart-Magos, C.; Leach, S. *J. Chem. Phys.* **1976**, *64*, 4006.

(35) Gaussian 94, Frisch, M. J.; Trucks, G. W.; Schlegel, H. B.; Gill, P. M. W.; Johnson, B. G.; Robb, M. A.; Cheeseman, J. R.; Keith, T. A.; Peterson, G. A.; Montgomery, J. A.; Raghavachari, K.; Al-Laham, M. A.; Zakrzewski, V. G.; Ortiz, J. V.; Foresman, J. B.; Cioslowski, J.; Stefanov, B. B.; Nanayakkara, A., Challacombe, M.; Peng, C. Y.; Ayala, P. Y.; Chen, W.; Wong, M. W.; Andres, J. L.; Replogle, E. S.; Gomperts, R.; Martin, R. L.; Fox, D. J.; Binkley, J. S.; Defrees, D. J.; Baker, J.; Stewart, J. P.; Head-Gordon, M.; Gonzales, C.; Pople, J. A., Gaussian, Inc.; Pittsburgh, PA, 1995.

(36) Williams, D. E. In *Reviews in Computational Chemistry*; Boyd, D. B., Lipkowitz, K. B., Eds.; VCH: New York, 1991; Vol. 2.

(37) Menapace, J. A.; Bernstein, E. R. *J. Phys. Chem.* **1987**, *99*, 2533.

(38) McGuire, R. F.; Momany, F. A.; Scheraga, H. A. *J. Phys. Chem.* **1972**, *76*, 375.

(39) Karasawa, N.; Dasgupta, S.; Goddard, W. A. *J. Phys. Chem.* **1991**, *95*, 2260.

(40) Momany, F. A.; Carruthers, L. M.; McGuire, R. F.; Scheraga, H. A. *J. Phys. Chem.* **1974**, *78*, 1595.

(41) *Molecular Vibrations, Theory of Infrared and Raman Vibrational Spectra*; Wilson, E B., Jr., Decius, J. C., Cross, P. C., Eds.; McGraw-Hill: New York, 1955.

(42) Li, S.; Bernstein, E. R. *J. Chem. Phys.* **1991**, *95*, 1577.

(43) Bray, J. A.; Bernstein, E. R. *J. Phys. Chem.*, **1998**, 102, preceding paper in this issue.

(44) Sun, S.; Bernstein, E. R. *J. Chem. Phys.* **1995**, *103*, 4447.

(45) Schauer, M.; Bernstein, E. R. *J. Chem. Phys.* **1985**, *82*, 726.

(46) Schauer, M.; Law, K. S.; Bernstein, E. R. *J. Chem. Phys.* **1985**, *82*, 736.

(47) Sun, S.; Bernstein, E. R. *J. Am. Chem. Soc.* **1996**, *118*, 5086.